Delgado Muñoz, D.; Sanchis, R.; Solsona Espriu, BE.; Concepción Heydorn, P.; López Nieto, JM. (2020). Influence of the Nature of the Promoter in NiO Catalysts on the Selectivity to Olefin During the Oxidative Dehydrogenation of Propane and Ethane. Topics in Catalysis. 63(19-20):1731-1742. https://doi.org/10.1007/s11244-020-01329-5

Influence of the nature of the promoter in NiO catalysts on the selectivity to olefin during the oxidative dehydrogenation of propane and ethane

by

Daniel Delgado [a], Rut Sanchis [b], Benjamín Solsona [b*], P. Concepción [a], José M. López Nieto [a*]

[a] Instituto de Tecnología Química, UPV-CSIC, Campus de la Universidad Politécnica de Valencia, Av. Naranjos s/n, 46022 Valencia, Spain.

[b] Departamento de Ingeniería Química, Universitat de Valencia, c/ Dr. Moliner 50, 46100, Burjassot, Spain.

* To whom correspondence should be addressed: FAX: +34963877809

Email address: jmlopez@itq.upv.es; benjamin.solsona@uv.es

Abstract

A comparative study of the catalytic properties for the oxidation of C_2-C_3 alkanes and olefins has been carried out over unpromoted and M-promoted NiO catalysts (Me= K, La, Ce, al, Zr, Sn, Nb). The catalysts have been characterized by several physico-chemical techniques (UV Raman, Visible Raman, FTIR of adsorbed CO and XPS). The characteristics of promoter elements are of paramount importance, since they are able to modify both the nature of the active nickel and the concentration of electrophilic O_2^-/O^- oxygen species. Thus, a relatively high acidity and valence of the promoter oxide (with oxidation state higher than +3) are necessary to achieve high selectivity to olefins during the oxidative dehydrogenation (ODH) of C_2-C_3 alkanes. In addition, an inverse correlation between the selectivity to the corresponding olefin and the concentration of electrophilic oxygen species has been observed, although the selectivity to propene during propane ODH is lower than the selectivity to ethylene achieved during ethane ODH. On the other hand, a very low influence of alkane conversion on the selectivity to the corresponding olefins is observed. This behaviour can be explained by considering that the reaction rate for olefin combustion are lower to the reaction rate for alkane oxidation. However, the comparative study of the oxidation of alkanes and olefins suggest that the differences observed between the ODH of propane and ethane are not related to the reactivity of olefins, but to the different number and reactivity of C-H bonds in both alkanes. A discussion on the importance of the concentration of active sites and the characteristics of the alkanes fed on the selectivity to olefin during the alkane ODH is also presented.

Keywords: propane; ethane; oxidative dehydrogenation; olefins; promoters; nickel oxide.

Declarations

Funding 'Not applicable'

Conflicts of interest/Competing interests 'Not applicable'

Availability of data and material. 'Not applicable'

Code availability 'Not applicable'

INTRODUCTION

Short chain olefins, especially ethylene and propylene, are undoubtedly the most important raw materials for the petrochemical industry, and perhaps also for the chemical industry in general [1]. These olefins constitute the fundamental pieces from which a multitude of chemical compounds are obtained.

Propylene is a highly versatile compound since can be obtained through different ways and can be transformed into a large number of industrial products. It is mainly obtained by steam cracking or fluid catalytic cracking (FCC) [2], but also by propane dehydrogenation (PDH) [3] and metathesis [4]. Currently, the new trends in steam cracking, especially in US, indicate a growth in the use of ethane (obtained from natural gas) as a feedstock at the expense of naphtha. The use of ethane implies a higher ethylene production and a sharp diminution of propylene production. Therefore, in order to cope with this increasing demand of propylene (ca. 10% in US in the past 3 years) [5], other "on-purpose propylene" (OPP) technologies, such as the non-oxidative dehydrogenation of propane, olefin metathesis and methanol to olefins (MTO) processes, have been industrially implemented [6].

The oxidative dehydrogenation (ODH) of propane could be an interesting alternative to steam cracking and non-oxidative dehydrogenation of propane, since from an energetic point of view, ODH is a much more favorable process, due to its exothermic character [7]. Besides, the presence of molecular oxygen in the feed permits an *in situ* regeneration of the active sites and prevents coke formation [8].

In terms of selectivity to propylene, one of the most efficient materials reported for the ODH of propane are supported vanadium oxide catalysts (ca. 90 % selectivity to propylene at low propane conversion) [8-12]. Unfortunately, yields to propylene described in literature are generally lower than 30%, due to olefin deep oxidation into

carbon oxides at increasing propane conversions [9]. Importantly, the acid-basic character of the support has to be controlled, so that basic supports are preferred to favor the propylene desorption [12].

Supported vanadium oxide catalysts were reported to be also efficient for ODH of ethane to ethylene [13-16], although they present the same disadvantage, i.e. the olefin formed readily decomposes by deep oxidation. In contrast with the optimal catalysts in the ODH of propane, optimal supports for the ODH of ethane present a rather acidic character [12-16].

Interestingly, the use of optimized promoted NiO catalysts [17-22] in the ODH of ethane has allowed the minimization of the ethylene decomposition into carbon oxides, this way achieving high olefin yields (> 40%), especially after the first publication by Lemonidou et al. [17]. However, not every promoter improves the catalytic performance of nickel oxide, the nature of the dopant element being of paramount importance. Basic promoters lead to the predominant formation of carbon oxides, whereas those with an acidic character show high selectivity to ethylene [18].

Unlike vanadium oxide catalysts [8-16], there are very few studies related to propane ODH over NiO-based catalysts [23-28]. Moreover, reports comparing the catalytic performance in ethane and propane ODH for NiO-based catalysts are even more scarce [28, 29].

Overall, most of the works published with nickel oxide catalysts use cerium as a promoter due to its high oxygen storage capacity and concentration of oxygen vacancies. In this way, several authors propose Ni-Ce-O catalysts as relatively selective in ODH of propane [23-26]. The best catalytic results were obtained by a catalyst with an excess of cerium (Ni/Ce atomic ratio of 0.5) and the authors ascribed the optimal results to the presence of highly dispersed nickel oxide species and a high concentration of anionic vacancies.

Nevertheless, the study of the influence of the characteristics of dopants in promoted NiO catalysts has not been undertaken so far.

In addition, the selectivity to propylene during propane ODH over NiO-based catalysts is lower than that achieved during the ethane ODH. However, it is not clear what are the key aspects for ethane ODH that are not met for the propane ODH.

In the present article, we want to study if this positive behavior observed in the ODH of ethane with NiO-based materials can also take place in the ODH of propane. Thus, the objective of this work is: i) to analyze if a similar improvement in the selectivity to the olefin takes place when NiO is modified by the addition of specific promoters [18]; ii) to determine, for propane ODH, the nature of the optimal dopants; and, iii) to compare the reactivity of C_2 and C_3 alkanes and their corresponding olefins (ethylene and propylene), in order to evaluate the contribution of consecutive reactions to the selectivity profiles. For this purpose, promoted NiO catalysts, considering a set of dopants with different physicochemical characteristics and acidities (i.e. K-, Ce-, Zr-, La-, Nb-, Sn-promoted catalysts) have been prepared, characterized and tested in the ODH of propane. For comparison the same catalysts have been tested in the ODH of ethane. The results are discussed in terms of the effect of promoters on the chemical nature of surface oxygen sites, and the derived catalytic consequences.

2. EXPERIMENTAL

2.1. Preparation of catalysts

Promoted NiO catalysts have been prepared through the evaporation of an ethanolic solution of nickel nitrate, a salt of the promoter, and oxalic acid using a (Ni+M)/oxalic acid molar ratio of 1 (the M-salts employed are shown in supporting

information). The paste obtained was dried in a furnace at 120ºC for 12 h and then calcined in air at 500ºC for 2h. The characteristics of the catalysts are shown in Table 1.

The samples have been called as M-NiO, Me being the promoter (K^+, Al^{3+}, Ce^{3+}, La^{3+}, Zr^{4+}, Sn^{4+} or Nb^{5+}). The amount of promoter has been fixed in M/(M + Ni) atomic ratio of 0.08, as this is close to the optimal ratio in promoted NiO catalysts for ethane ODH [18]. For comparison, an unpromoted nickel oxide (i.e. uNiO) was also studied.

2.2. Characterization techniques

Catalyst surface areas were determined by multi-point N_2 adsorption at 77 K, in a Micromeritics ASAP 2000 instrument. The data were treated in accordance with the BET method.

Average chemical composition of catalysts was determined by inductively coupled plasma atomic emission spectroscopy (ICP-AES).

Powder X-ray diffraction (XRD) was used to identify the crystalline phases present in the catalysts. An Enraf Nonius FR590 sealed tube diffractometer, with a monochromatic CuKa1 source operated at 40 kV and 30 mA was used. The particle sizes have estimated from XRD data using the Scherrer formula. This formula has been applied to peaks related to (101), (012), (113), and (024) crystal planes of NiO.

Raman spectra were collected in an inVia Renishaw spectrometer equipped with an Olympus microscope. The measurements were carried out at different wavelengths: 325 (UV-Raman) and 514 nm (Visible-Raman).

IR spectra of adsorbed CO were recorded at low temperature (-176ºC) with a Nexus 8700 FTIR spectrometer, at a spectral resolution of 4 cm^{-1}, using a DTGS detector. An IR cell allowing in situ treatments in controlled atmospheres and temperatures from -176 ºC to 500 ºC has been connected to a vacuum system with gas dosing facility. Self-

supporting wafers were initially pre-treated at 250 ºC/1.5 h (in an oxygen flow, 20 ml min^{-1}), followed by evacuation at 300ºC/1h (at 10^{-4} mbar), and cooled down to -176ºC (under dynamic vacuum). Finally, CO was adsorbed by CO dosing at increasing pressure (0.4-8.5 mbar), and IR spectra were recorded after each dosage.

X-ray photoelectron spectra were collected using a SPECS spectrometer with a MCD-9 detector and using a non-monochromatic AlKa (1486.6 eV) X-ray source. Spectra were recorded using analyzer pass energy of 50 eV, an X-ray power of 200 W, and under an operating pressure of 10^{-9} mbar. During data processing of the XPS spectra, binding energy (BE) values were referenced to C1s peak (284.5 eV). Spectra treatment has been performed using the CASA software.

2.3. Catalytic tests

The catalytic experiments were carried out at atmospheric pressure in a tubular isothermal fixed bed reactor, at atmospheric pressure, working in the 250-350 ºC temperature range. Catalyst sample (0.3-0.5 mm particle size) were introduced in a quartz reactor diluted with silicon carbide in order to keep a constant volume. Typically, 0.1 g of catalyst and a flow rate of reactants of 50 ml/min were used, although both the catalyst amounts loaded and the total flows used were varied to achieve different hydrocarbons conversions at a fixed reaction temperature. The feed corresponds to a mixture consisting of C_3/O_2/He with a molar ratio of 10/10/80. For comparison, some experiments were undertaken in the oxidation of ethane, propylene or ethylene using a feed consisting of a mixture of hydrocarbon/O_2/He with a molar ratio of 10/10/80. Reactants and reaction products have been analysed using a gas chromatograph equipped with two packed columns: (i) molecular sieve 5 Å (2.5 m); and (ii) Porapak Q (3 m). Olefins (propylene or ethylene), water and carbon dioxide were the main reaction products detected from alkanes (propane

or ethane, respectively). CO could be identified in a couple of catalysts but with selectivity lower than 0.2%. Blank runs in the absence of catalyst were carried out until 450ºC. Zero conversion was observed in both C_2-C_3 alkane ODH and C_2-C_3 olefin oxidation in blank experiments.

3. RESULTS AND DISCUSSION

3.1 Catalysts characterization

Table 1 shows some physicochemical and catalytic properties for propane oxidation of unpromoted (uNiO sample) and M-promoted nickel oxide catalysts (M-NiO; M= K, La, Ce, Al, Zr, Sn, Nb). XRD patterns of the catalysts show the only presence of cubic phase of NiO (JCPDS: 47-1049), although low intensity lines corresponding to other phases were observed in the case of Ce-, La- and Zr-promoted materials (Fig. S1, supporting information). On the other hand, the incorporation of promoters to NiO leads to a decrease of NiO crystallite size, and a subsequent increase in catalyst surface area (Table 1). This way, uNiO sample presents a mean crystallite size of NiO of 35 nm, while for promoted catalysts NiO crystallite size ranges from 9 to 17 nm.

The series of promoted NiO catalysts was characterized by Raman spectroscopy (Fig. 1). Figure 1A shows Raman spectra collected at an irradiation wavelength of 514 nm. Unpromoted NiO shows the characteristic vibrational features of nickel oxide, displaying a band centered at ca. 495 cm^{-1} (Fig. 1A, spectrum a) [30]. Interestingly, depending on the nature of the promoter, two different trends are observed in the Raman spectra. Except for K^+-promoted NiO catalysts (Fig. 1A, spectrum b), which shows a similar Raman profile than uNiO, band-broadening is observed for all promoted NiO catalysts (Fig. 1A, spectra c to d). This fact suggests that one common effect of adding high oxidation state dopants is to promote a loss of order in NiO, likely due to the presence

of defects. In addition, a shift to higher frequencies is observed for Ni-O modes in some promoted NiO catalysts (from 495 cm^{-1} to 510-589 cm^{-1}, for Ce-, Sn-, Zr- and Nb-promoted materials), indicating changes in the Ni-O bond nature, likely due to the partial incorporation of M^{n+} species within NiO crystal lattice (**Fig. 1A**, spectra d to g).

Figure 1

Figure 1. Raman spectra of NiO-based catalysts recorded at an irradiation wavelength of 514 nm (A) and 325 nm (B). Samples: a) uNiO; b) K-NiO; c) La-NiO; d) Ce-NiO; e) Zr-NiO; f) Sn-NiO; g) Nb-NiO. Characteristics of catalysts in Table 1.

In order to shed some light on the vibrational characteristics of the catalysts, the materials were further analyzed by UV Raman, by irradiating the samples with a UV-laser (i.e. 325 nm) (Fig 1B). This technique has been reported to be more sensitive to the surface features of solid materials, thus being more suitable for the study of heterogeneous catalysts [31-33]. All the catalysts show typical UV Raman features of NiO: one-phonon transversal optical (TO) and longitudinal optical (LO) modes at ca. 568 cm^{-1} (1P); and two-phonon modes 2TO (at ca. 725 cm^{-1}), TO+LO (at ca. 897 cm^{-1}) and 2LO (at ca. 1110 cm^{-1}) (Fig. 1B) [34]. The relative intensity of these signals can provide information on the structural disorder and particle size of NiO. The lowest relative intensity of defect-induced one-phonon signal (1P, at ca. 568 cm^{-1}) is observed for unpromoted NiO and K^{+}-promoted catalysts (Fig. 1B, spectra a and b). On the contrary, NiO catalysts promoted with elements showing higher oxidation states (La^{3+}, $Ce^{3+/4+}$, Zr^{4+} or Nb^{5+}) present a substantially higher intensity of this 1P mode (Fig. 1B, spectra c to g). This increase in the relative intensity of one-phonon mode observed by UV Raman can be explained in terms of the following features induced by the incorporation of promoter: i) a smaller NiO

particle size [35]; ii) the presence of a higher concentration of defects [36]; and, iii) a higher structural disorder [37].

FTIR of adsorbed CO have been also undertaken in order to study the Lewis acidity of the surface of the catalysts [38], in a manner that strong acid sites arise at high frequencies, whereas weak acid sites arise at low frequencies. Taking this into account, and according to the results of Table 1 (see also Fig. S2 in supporting information), the strength of acid sites in our catalysts increases in the order [18]: K-NiO << uNiO < La-NiO < Al-NiO ~ Zr-NiO < Sn-NiO < Nb-NiO. Similarly, the number of acid sites follows the order: Nb-NiO > Sn- NiO > Zr- NiO > La- NiO > Al- NiO > NiO, K- NiO.

A detailed XPS study was also conducted in order to get insights into surface features of NiO-based catalysts. As electrophilic O_2^- and O^- oxygen species can be directly involved in total oxidation reaction pathways, the nature of surface oxygen sites has been studied (Table 1). Figure 2 shows O1s core-level XPS spectra of promoted NiO catalysts. All the spectra can be fitted to three single peaks, centered at ca. 528, 531 and 533 eV, which can be assigned to lattice O^{2-}, OH^-, and electrophilic (O_2^- and O^-) oxygen species, respectively [39].

Figure 2

Figure 2. O1s XPS spectra of catalysts: a) uNiO; b) K-NiO; c) La-NiO; d) Ce-NiO; e) Zr-NiO; f) Sn-NiO; g) Nb-NiO.

Interestingly, differences in the relative intensity of these signals are clearly observed depending on the nature of the promoter. For instance, the incorporation of a low oxidation state promoter like K^+ leads to an increase in the relative intensity of the signal assigned to electrophilic O^- species (Fig. 2, spectrum b) with respect to undoped

uNiO catalyst (Fig. 2, spectrum a). These electrophilic sites are those reported to be responsible for total oxidation of alkanes [40, 41]. However, the relative intensity of this signal decreases notably when metal cations with an oxidation state higher than 2+ are incorporated (i.e. Nb^{5+}, Zr^{4+}, La^{3+}, etc.) (Fig. 2, spectra c to g). The surface concentration of O^- sites on promoted nickel oxide catalysts has been estimated (Table 1). Then it has been observed that the concentration of surface electrophilic O^- sites decreases from ca. 22.9 at.% in K-NiO catalyst down to 6.6 at.% in Nb-NiO catalyst.

3.2. Catalytic results in the oxidative dehydrogenation of propane

The main reaction products observed in the oxidation of propane using NiO-based catalysts have been propylene and CO_2. Partially oxygenated hydrocarbons were not detected and CO was only observed as traces.

Figure 3 shows comparatively propane conversion and selectivity to propylene achieved during the ODH of propane for the different NiO-based catalysts at 325ºC. For comparison, the selectivity to propylene achieved with promoted NiO catalysts at a propane conversion of 10% is shown in Table 1. The most active catalyst was that with cerium, whereas that with potassium achieved the lowest activity. Thus, the order of catalytic activity observed is as follows: Ce-NiO > La-NiO > Zr-NiO > Al-NiO > uNiO > Nb-NiO > Sn-NiO >> K-NiO. Moreover, the selectivity to propylene follows a different trend: Nb-NiO > Zr-NiO, Sn-NiO > Al-NiO, La-NiO > Ce-NiO >> uNiO > K-NiO. Interestingly, promoted NiO catalysts present a selectivity to propylene higher than undoped (uNiO) or K-doped (K-NiO) catalysts; with Nb-promoted NiO presenting the highest values of selectivity to propylene (ca. 45%), whereas uNiO and K-NiO samples present the lowest ones (16 and 11% respectively).

Figure 3

Figure 3. Propane conversion (■) and selectivity to propylene (■) for unpromoted and promoted NiO catalysts in the ODH of propane. Reaction conditions: 325ºC, W/F = 8 g_{cat} h /mol_{C3}. Remaining conditions in the Experimental section. For Ce-NiO W/F = 2 g_{cat} h /mol_{C3}.

3.3. Relationship between the nature of the promoter and the characteristics of the catalysts with the selectivity to propylene.

The acid characteristics of the NiO-based catalysts can have an important influence on the adsorption and desorption of reactants and reaction products, and therefore on the catalytic performance. Thus, with the aim of understanding the catalytic results over promoted catalysts, we have attempted to correlate the selectivity to propylene with the acid characteristics of the catalysts (Fig. 4), considering the results achieved by FTIR from adsorbed CO (Table 1 and Fig. S2). According to these results, the higher the amount and strength of Lewis acid sites on the NiO-catalysts, the higher the selectivity to propylene (obtained in the ODH of propane) (Fig. 4).

Figure 4

Figure 4. Variation of the selectivity to propylene at 10% conversion and 350ºC with the amount of adsorbed CO (FTIR). Note: Adsorbed CO total FTIR is the total number of surface acid sites calculated as the number of CO molecules adsorbed on each site.

We must inform that a similar trend was observed during the ODH of propane and ethane on similar catalysts [18]. However, in the case of the ODH of ethane the selectivity to the olefin was substantially higher than in the ODH of propane (Fig. S3). Then, a selectivity to ethylene up to 85-90 % over Nb-NiO and Sn-NiO catalysts have been achieved.

Figure 5 displays the variation of the selectivity to the olefin during the ODH of propane or ethane as a function of the surface concentration of electrophilic O^- sites. A drop of the selectivity to the olefin is observed when the amount of electrophilic sites increases. Then, the proportion of electrophilic sites for the least selective catalyst (i.e. K-NiO) is 23% whereas for the most selective catalyst (i.e. Nb-NiO) is only of 6.6 at.%. This fact suggests that it is possible to eliminate non-selective oxygen sites on NiO by the incorporation of promoters. Interestingly, such a NiO-promoter interaction can take place either by the incorporation of the promoter within NiO framework (as in Nb-NiO) [17-22, 42], or by intimate contact between separated oxide phases (as in Sn-NiO) [42].

Figure 5

Figure 5. Influence of amount of electrophilic O^- sites (determined by XPS) on the selectivity to propylene, during the ODH of propane (○), or on the selectivity to ethylene, during the ODH of ethane (●). Data at 10% alkane conversion and a reaction temperature of 350ºC. Catalytic results for propane ODH (this study), using a C_3/O_2/He molar ratio of 10/10/80; Catalytic results for ethane ODH (from ref. 18), using a C_2/O_2/He molar ratio of 10/3.3/86.7.

It can be stated that, for NiO-based catalysts, high valence promoters (like Nb^{5+}, Sn^{4+} or Zr^{4+}) [17-20, 42-45], or the use of supports [46, 47], tend to remove unselective electrophilic O^- species Thus, the highest selectivity to propylene from propane (but also ethylene from ethane) is observed with catalysts displaying the lowest amount of electrophilic species. These results go in line with previous reports on ethane ODH, which show that the selectivity to ethylene increases concomitantly with a decrease in the number of Ni neighbours in the first (Ni-O) and second coordination shell (Ni-Ni) for supported NiO catalysts [46]. In addition, it has been also suggested that the incorporation of promoters and supports/diluters leads to a decrease of the average oxidation state of Ni^{n+} sites, and to a decrease in the concentration of non-selective electrophilic oxygen

sites on the surface, likely to occur due to the elimination of non-stoichiometric Ni^{3+} surface sites [42].

In this way, it can be interesting to indicate that the lowest relative intensity of defect-induced one-phonon (1P mode) signal determined by UV Raman is observed for unpromoted NiO and K^{+}-promoted catalysts (Fig. 1B, spectra a and b), which are those showing the lowest selectivity in ODH. On the contrary, the higher intensity of this 1P mode in the UV Raman (Fig. 1B, spectra c to g) is observed in NiO catalysts promoted with elements showing higher oxidation states (La^{3+}, $Ce^{3+/4+}$, Zr^{4+} or Nb^{5+}), which present a higher selectivity to olefins in ODH reactions.

3.4. On the reactivity of alkanes and olefins in oxidation reactions over NiO-based catalysts

In the case of propane oxidation, only propylene and CO_2 are produced (Tables S1-S3), which can be considered as primary reaction products. This behaviour is similar than that observed for ethane oxidation in which ethylene and CO_2 are the main reaction products. CO was observed only as traces in both cases.

For this reason, and in order to evaluate the contribution of consecutive reactions, Figure 6 shows the variation of the selectivity to olefin during the ODH of propane (Fig. 6A) and ethane (Fig. 6B) at 350ºC for some representative catalysts, i.e. Nb- and Zr-promoted and unpromoted NiO catalysts (fixing the reaction temperature and modifying the contact time).

Figure 6

Figure 6. Variation of the selectivity to olefin with the alkane conversion at 350ºC during the ODH of propane (A) or the ODH of ethane (B) on Ni-based catalysts: uNiO; Zr-NiO and Nb-NiO. Remaining reaction conditions in text.

The selectivity to ethylene (during ethane ODH) is higher than the selectivity to propylene achieved during propane ODH. However, in both cases, a low influence of the alkane conversion on the selectivity to the corresponding olefin is observed over the studied catalysts. Thus, the consecutive deep oxidation of the olefins should be very low with respect to the formation of olefins during the ODH reaction. This behavior is completely different to that achieved over supported vanadium oxide catalysts [12-16, 48-50], in which it is well known that the alkane conversion has a strong influence on the selectivity to olefins.

To confirm this trend, a comparative study on the oxidation of C_2 and C_3 alkanes and their corresponding olefins (i.e. ethylene and propylene) has been carried out on three selected catalysts, i.e. uNiO, Zr-NiO and Nb-NiO, at the same reaction conditions (350ºC, using a hydrocarbon/oxygen/helium molar ratio of 10/10/80 and a contact time, W/F, of 8.2 g_{cat} h/$(mol_{hydroc})^{-1}$) (Tables S1-S3). Figure 7 presents the reaction rate for alkane (r_{-C2H6} or r_{-C3H8}) or olefin (r_{-C2H4} or r_{-C3H6}) conversion as well as the reaction rate for the formation of the main reaction products (r_{C3H6}, r_{C2H4}, r_{CO2} and r_{CO}). In all cases, the reaction rate for hydrocarbon conversion decreases according to: Zr-NiO > uNiO > Nb-NiO. However, when considering the specific reaction rate (i.e. considering the surface area of catalysts) for ethane and propane oxidation, the catalytic activity decreases according to: uNiO > Zr-NiO > Nb-NiO. In addition, there exist common features in the reactivity when comparing the reaction rate for the conversion of the alkane and alkene for C_2 and C_3 substrates. Thus, in all cases, the reaction rate for the olefin transformation is lower than that for the corresponding alkane, being this difference greater in the case of C2 hydrocarbons than for C3 hydrocarbons. Indeed, the relative reaction rates for

ethylene/ethane is ca 0.5 (more specifically, 0.51 for uNiO; 0.53 for Zr-NiO and 0.42 for Nb-NiO), whereas the relative reaction rates for propylene/propane it is *ca.* 0.70 (more specifically, 0.69 for uNiO; 0.64 for Zr-NiO and 0.80 for Nb-NiO) (see Table 2). These values are very different to those reported for supported vanadium oxide catalysts, in which the ratio between olefin/alkane oxidation is between 4 to 10 [16]. Thus, the results presented here confirm the low influence of alkane conversion on the selectivity to olefin during ODH of ethane or propane on NiO-based catalysts. In addition, regardless of the catalyst (see Fig. 7, for C_2H_4 and C_3H_6), the activity for propylene oxidation is slightly higher than for ethylene oxidation.

On the other hand, no major differences are observed between the reaction rates for alkanes and olefins oxidation when comparing more selective (such as Nb-or Zr-promoted NiO) or less selective (unpromoted NiO) catalysts for alkane ODH. This suggests that: i) the differences in selectivity to olefins during the ODH of ethane and propane depend largely on the characteristics of the fed alkane and not on the reactivity of the olefins; and ii) the presence or absence of promoted in NiO-based catalysts has a very low influence on the deep oxidation of olefins.

Figure 7

Figure 7. Reaction rate for hydrocarbon conversion (r_{-C2H6}, r_{-C3H8}, r_{-C2H4} or r_{-C3H6}) as well as the reaction rate for the formation of the main reaction products (r_{C3H6} or r_{C2H4}, r_{CO2} and r_{CO}) during the oxidation of ethane (**a**), ethylene (**b**), propane (**c**), and propylene (**d**) over NiO, Zr-NiO and Nb-NiO catalysts at 350ºC. Experimental conditions as in table S1-S3).

Accordingly, the differences observed for undoped and doped NiO catalysts during the propane and ethane ODH are much more related to changes in the ratio between the olefin formation and the CO_2 formation from each alkane (which probably is related to the

different C-H and C-C bond strengths in both alkanes) rather than changes in the olefin deep oxidation over each catalyst.

General remarks and comparison between propane and ethane ODH

The nature of the promoter highly affects the catalytic performance in the ODH of propane over NiO-based catalysts (in a parallel trend to that observed for ethane [18]). As observed previously for ethane ODH [17-22, 43-47], those promoters with high oxidation state and high acidity lead to the best catalytic results as this minimizes the presence of surface electrophilic O_2^- and O^- oxygen species [43], especially when using Nb^{5+} as promoter [17, 19, 42-45].

In our case, niobium promoted NiO sample resulted to be the most efficient catalyst. The positive role of acidity in promoted NiO catalysts, especially for propane ODH, contrasts with the results observed for supported vanadium oxide catalysts in which the presence of acid sites has detrimental influence for obtaining high propylene yields [12, 16]. In fact, among vanadium based catalysts, K-doped VO_x/Al_2O_3 [12, 48] or V-Mg-O [49] have been reported as selective in propane ODH, whereas VO_x/Al_2O_3 [13,14, 48, 49] is more selective in ethane ODH.

Accordingly, the selectivity to olefins during C_2-C_3 alkane ODH seems to be mainly related to the nature of the active sites (and in the ratio between electrophilic and nucleophilic oxygen species), whereas the deep oxidation of olefins on NiO-based catalysts seems to be very low (and similar independently of the presence or absence of promoters) as concluded from results in Figure 7.

However, the selectivity to ethylene during the ethane ODH is remarkably higher than that observed for the selectivity to propylene during propane oxidation (Figures 5 and 6). Thus, on Nb-NiO catalyst, the selectivity to the olefin in the ODH of ethane is

over 80%, whereas in the ODH of propane is only of ca. 45%. Similarly, over unpromoted NiO catalyst the selectivity to ethylene is 40-45%, whereas that to propylene is ca. 16%.

In agreement to previous results [17-22, 43-47], a general reaction scheme for the oxidative dehydrogenation of propane and ethane on nickel oxide catalysts involves the direct transformation of propane or ethane into propylene or ethylene but also the direct formation of CO_2 from either propane or ethane (Fig. 8). Thus, according to the results shown in Fig. 7 and Table 2, the selectivity to olefins strongly depends on the k_2/k_1 ratio (i.e. parallel reactions which strongly depend on both the characteristics of catalyst an the alkane feed). However, in all cases, the consecutive reactions (with low k_3/k_1 ratio) has a low importance on the selectivity to olefins. On the other hand, the formation of CO is negligible from alkanes and very low from olefins.

A last question to be considered is the fact that the selectivity to olefin during the ODH of ethane is higher than that achieved during ODH of propane, when relatively small differences in the k_3/k_1 ratio are concluded. In fact, it has been observed that the ratio between the reaction rate for olefin and alkane oxidation is ca. 0.5 ($r\text{-}_{C2H4}$/ $r\text{-}_{C2H6}$) and 0.7 ($r\text{-}_{C3H6}$/ $r\text{-}_{C3H8}$) (Table 2), suggesting a low influence of the deep oxidation of olefins during the alkane ODH in both unpromoted and promoted NiO-based catalysts.

Figure 8

Figure 8. Reaction pattern of the ODH of propane and ethane on NiO based catalysts.

In fact, the reaction rate for deep oxidation of propylene would be expected to be greater than that of ethylene, since the stability of propylene (presenting weak C-H allylic bonds) is supposed to be lower than that of ethylene (presenting stronger C-H vinylic bonds). [51]. In addition, the adsorption constant of ethylene on NiO is considerably lower than

that of propylene [52, 53], which apparently would decrease the extent of the ethylene decomposition. However, and although this can be the case of the ODH over V-containing catalysts, this does not take place for NiO-based catalysts. Thus, unexpectedly, the higher olefin yields achieved in the ODH of ethane with respect to those achieved during propane ODH are not due to the differences in the stability of the olefins (since in both cases the reaction rate for olefin oxidation is lower than that for alkane oxidation), but to the tendency of propane to be more easily transformed into carbon dioxide.

Yao and Kreamer in 1973 [28] reported a catalytic behavior for the oxidation of C_2-C_4 hydrocarbons on pure NiO catalysts similar to the trend presented here. These authors observed that, unexpectedly, the catalytic activity for alkane oxidation was higher than for olefin oxidation. This is especially surprising in the case of propylene since, despite showing weaker allylic C-H bonds, it is less reactive than propane (with stronger primary and secondary C-H bonds), and even less reactive than a stable molecule as ethane. The interesting results presented here verify that this trend occurs not only for the unselective NiO (with low selectivity to olefins during the ODH of ethane and propane), but also on promoted NiO catalysts. Thus, NiO catalysts promoted with Nb^{5+} or with Zr^{4+} present high selectivity to olefin, especially during the ODH of ethane, and to a less extent during the ODH of propane, but both undoped and doped NiO catalysts present similar reaction rates for deep oxidation of C_2-C_3 olefins (Fig. 7, b and d).

The results obtained here suggest that the selective sites for ethane or propane ODH hardly intervene (their contributions is very low) in the combustion of olefins. Therefore, and in agreement with previous results [17, 42, 43], there must be two types of centers involved in the alkane ODH: i) selective sites for olefin formation, which are strongly related to the presence of the promoter (especially in the case of Nb); and ii) non-selective sites, favoring the formation of CO_2, which are majority in the case of pure NiO.

On the other hand, and in agreement to previous reported mechanism, the alkane ODH involves three different steps: i) for ethane ODH, in which the scission of C-H bond is the rate-determining step [43]; ii) ethane deep oxidation, in which the rate-determining step may be either the adsorption of ethane as C_2H_5 radical with breaking of the C-H bond if the slow step is the chemisorption of the ethane molecules, or the interaction between the adsorbed O_2 and either gas phase or physically adsorbed C_2H_6 through attack at the C-H bond [28]; iii) ethylene deep oxidation, minority on NiO-based catalysts, in which the rate of adsorption of ethylene or reaction between oxygen and the double bond of ethylene (adsorbed on the surface, with the C_2H_4 molecules adsorbed on the surface through the π bond) may be the rate-determining step [28].

Finally, the lower selectivity to propylene over promoted catalysts, when comparing with the catalytic results for ethane ODH, could be related to the different number and dissociation energies of C-H bonds present in ethane and propane molecules, as suggested by Iglesia et al. [14].

In the present article, it has been clearly observed for both ethane and propane ODH that the selectivity to carbon dioxide increases with the surface concentration of O^- electrophilic sites. As the selectivity to olefins hardly falls with the alkane conversion, it indicates that these unselective sites are more reactive in the alkane oxidation than in the olefin oxidation. In the case of Nb-NiO catalyst 6.6% of the surface oxygen is O^- electrophilic sites, which leads to an initial selectivity to CO_2 of 10-15% in the ODH of ethane and 45-50% in the ODH of propane. In the case of Zr-NiO catalyst 11% of O^- surface electrophilic sites lead to an initial selectivity to CO_2 of 25-30% and ca. 60% for ODH of ethane and propane respectively. In the unpromoted NiO catalyst 16% of surface electrophilic sites lead to an initial selectivity to CO_2 of 45-50% and ca. 85% for ODH of ethane and propane respectively. All these data indicate that in all catalysts for each 1%

of O^- sites the selectivity to CO_2 increases by 2-3 % in the ODH of ethane whereas increases by 5-7% in the ODH of propane. Accordingly, the combustion of propane takes place at a higher reaction rate than the combustion of ethane in the O^-surface electrophilic sites. It is possible that the higher size and the greater number of C-H bonds in propane (compared to ethane) gives rise to a better attack of the unselective O^- species to the propane molecule, with the consequent higher formation of CO_2.

Interestingly, the formation of CO is not detected, neither from ethane nor from propane, and this is likely related to the high reaction rate of the CO oxidation to CO_2 on nickel oxide based catalysts, which could take place at temperatures below 150ºC [43], which are significantly lower than those required for the ODH of propane. Moreover, CO is usually a reaction product obtained as a result of the decomposition of the olefin and, for NiO-based catalysts, this step seems to be negligible, at least up to 20% alkane conversion.

Conclusions

Oxidative dehydrogenation of propane to propylene can be undertaken using promoted NiO catalysts achieving propylene yields of ca. 10% at low reaction temperatures (in the 300-350ºC range). The catalytic behaviour of unpromoted NiO is poor but can be improved, as well as the physicochemical properties, if NiO is modified by the incorporation of a second metal oxide.

Overall, the oxidation state of the promoter determine the interaction NiO-promoter affecting the size of the NiO particles and the acidity of the catalyst, and importantly the concentration of surface O^- electrophilic species. A clear inverse relationship has been observed between the selectivity to the olefin (in both cases from propane or from ethane) and the concentration of surface O^- electrophilic species. Then, the higher the amount of

these unselective O species the highest is the extent of the direct alkane combustion whereas the extent of the olefin decomposition is hardly affected.

The optimal catalytic results have been obtained by the catalysts in which the promoter metal presents high valence, as Nb^{5+}. Generally speaking, selective catalysts present tiny NiO crystallites and high acidity although the most determining factor seems to be the removal of unselective electrophilic O^- species. A link of all these characteristics is very likely. Nb-promoted NiO catalysts resulted to be the most efficient for the ODH of propane whereas the unpromoted NiO and K-doped NiO are the least selective to propylene.

On the other hand, a parallelism between the selectivity to ethylene observed in the ODH of ethane and the selectivity to propylene in the ODH of propane has been observed (the electrophilic O^- species are related to the direct combustion of the alkane), although the selectivity to ethylene achieved is significantly higher than the selectivity to propylene. However, the reaction rate for olefin combustion (ethylene or propylene) is lower than the reaction rate for alkane transformation, with the consequent high stability of olefins during the alkane ODH.

The lower selectivity to propylene (referred to that achieved for ethylene) cannot be explained by the different reactivity of olefins (very low in both olefins when comparing to the corresponding alkanes). Thus, the greater number of C-H bond in propane could facilitate a better attack of unselective oxygen species, favouring a higher formation of carbon dioxide.

Acknowledgements

The authors would like to acknowledge the Ministerio de Ciencia, Innovación y Universidades of Spain (RTl2018-099668-B-C21 and MAT2017-84118-C2-1-R

projects) and FEDER. Authors from ITQ also thank Project SEV-2016-0683 for supporting this research. D.D. thanks MINECO and Severo Ochoa Excellence Program for his fellowship (SVP-2014-068669).

References

1. Stangland EE (2018) Shale Gas Implications for C_2-C_3 Olefin Production: Incumbent and Future Technology. Annu Rev Chem Biomol Eng 9:341-364.
2. Corma A, Corresa E, Mathieu Y, Sauvanaud L, Al-Bogami S, Al-Ghrami MS, Bourane A (2017) Crude oil to chemicals: light olefins from crude oil. Catal Sci Technol 7:12-46.
3. Sattler JJHB, Ruiz-Martinez J, Santillan-Jimenez E, Weckhuysen BM (2014) Catalytic Dehydrogenation of Light Alkanes on Metals and Metal Oxides. Chem Rev 114:10613-10653.
4. Mol JC (2004) Industrial applications of olefin metathesis. J Mol Catal A-Chem 213:39-45.
5. https://www.eia.gov/dnav/pet/hist/LeafHandler.ashx?n=PET&s=MPLRX_NUS_1&f=M
6. https://www.acs.org/content/acs/en/pressroom/cutting-edge-chemistry/the-propylene-quandary.html
7. Ren T, Patel MK, Blok K (2008) Steam cracking and methane to olefins: Energy use, CO_2 emissions and production costs. Energy 33:817-833.
8. Cavani F, Ballarini N, Cericola A (2007) Oxidative dehydrogenation of ethane and propane: How far from commercial implementation? Catal Today 127:113-131.
9. Grabowski R (2006) Kinetics of Oxidative Dehydrogenation of C_2-C_3 Alkanes on Oxide Catalysts. Catal Rev 48:199–268.
10. Grant JT, Venegas JM, McDermott WP, Hermans I (2018) Aerobic Oxidations of Light Alkanes over Solid Metal Oxide Catalysts. Chem Rev 118:2769-2815.
11. Gärtner CA, van Veen AC, Lercher JA (2013) Oxidative Dehydrogenation of Ethane: Common Principles and Mechanistic Aspects. ChemCatChem 5:3196-3217.
12. Blasco T, López Nieto JM (1997) Oxidative dehydrogenation of short chain alkanes on supported vanadium oxide catalysts. Appl Catal A-Gen 157:117-142.
13. Argyle M D, Chen K, Bell AT, Iglesia E (2002) Effect of Catalyst Structure on Oxidative Dehydrogenation of Ethane and Propane on Alumina-Supported Vanadia. J Catal 208:139–149.
14. Zboray M, Bell AT, Iglesia E (2009) Role of C-H Bond Strength in the Rate and Selectivity of Oxidative Dehydrogenation of Alkanes. J Phys Chem C 113:12380–12386.

15. Rozanska X, Fortrie R, Sauer J (2014) Size-Dependent Catalytic Activity of Supported Vanadium Oxide Species: Oxidative Dehydrogenation of Propane. J Am Chem Soc 136:7751−7761.
16. Solsona B, Blasco T, López Nieto JM, Peña ML, Rey F, Vidal-Moya A (2001) Vanadium-Containing MCM-41 for Partial Oxidation of Lower Alkanes. J Catal 203:443–452.
17. Heracleous E, Lemonidou AA (2006) Ni–Nb–O mixed oxides as highly active and selective catalysts for ethene production via ethane oxidative dehydrogenation. Part I: Characterization and catalytic performance. J Catal 237:162-174.
18. Lopez Nieto JM, Solsona B, Grasselli RK, Concepcion P (2014) Promoted NiO Catalysts for the Oxidative Dehydrogenation of Ethane. Top Catal 57:1248-1255.
19. a) Zhu H, Rosenfeld DC, Harb M, Anjum DH, Hedhili MN, Ould-Chikh S, Basset JM (2016) Ni−M−O (M = Sn, Ti, W) Catalysts Prepared by a Dry Mixing Method for Oxidative Dehydrogenation of Ethane. ACS Catal 6:2852-2866; b) Zhu H, Dong H, Laveille P, Saih Y, Caps V, Basset JM (2014) Metal oxides modified NiO catalysts for oxidative dehydrogenation of ethane to ethylene. Catal Today 228:58–64.
20. Heracleous E, Lemonidou AA (2010) Ni-Me-O mixed metal oxides for the effective oxidative dehydrogenation of ethane to ethylene-Effect of promoting metal Me. J Catal 270:67–75.
21. Qiao A, Kalevaru VN, Radnik J, Martin A (2016) Oxidative dehydrogenation of ethane to ethylene over Ni–Nb–M–O catalysts: Effect of promoter metal and CO_2-admixture on the performance. Cat Today 264:144–151.
22. Sanchis A, Delgado D, Agouram S, Soriano MD, Vázquez MI, Rodriguez-Castellón E, Solsona B, Lopez Nieto JM (2017) NiO diluted in high surface area TiO_2 as an efficient catalyst for the oxidative dehydrogenation of ethane. Appl Catal A-Gen 536:18–26.
23. Jalowiecki-Duhamel L, Ponchel A, Lamonier C, D'Huysser A, Barbaux Y (2001) Relationship between Structure of $CeNi_XO_Y$ Mixed Oxides and Catalytic Properties in Oxidative Dehydrogenation of Propane. Langmuir 17:1511–1517.
24. Boizumault-Moriceau P, Pennequin A, Grzybowska B, Barbaux Y (2003) Oxidative dehydrogenation of propane on Ni-Ce-O oxide: effect of the preparation method, effect of potassium addition and physical characterization. Appl Catal A-Gen 245:55–67.

25. Li J-H, Wang C, Huang Ch, Sun Y, Weng W, Wan H (2010) Mesoporous nickel oxides as effective catalysts for oxidative dehydrogenation of propane to propene. Appl Catal A-Gen. 382:99–105.
26. Fang K, Liu L, Zhang M, Zhao L, Zhou J, Li W, Mu X, Yang Ch (2018) Synthesis of Three-Dimensionally Ordered Macroporous NiCe Catalysts for Oxidative Dehydrogenation of Propane to Propene. Catalysts 8:19.
27. Du K, Hao M, Li Zh, Hong W, Liu J, Xiao L, Zou Sh, Kobayashi H, Fan J (2019) Tuning catalytic selectivity of propane oxidative dehydrogenation via surface polymeric phosphate modification on nickel oxide nanoparticles. Chinese J Catal 40:1057–1062.
28. Yao YFY, Kummer JT (1973) The Oxidation of Hydrocarbons and CO Over Metal Oxides. I. NiO Crystals. J Catal 28:124-138.
29. Smolakova L, Capek L, Botkova S, Kovanda F, Bulanek R, Pouzar M (2011) Activity of the Ni–Al Mixed Oxides Prepared from Hydrotalcite-Like Precursors in the Oxidative Dehydrogenation of Ethane and Propane. Top Catal 54:1151–1162.
30. Dietz RE, Parisot GI, Meixner AE (1971) Infrared Absorption and Raman Scattering by Two-Magnon Processes in NiO. Phys Rev B 4:2302−2310.
31. Zhang J, Li M, Feng Z, Chen J, Li C (2006) UV Raman Spectroscopic Study on TiO_2. I. Phase Transformation at the Surface and in the Bulk. J Phys Chem B, 110:927-935.
32. Li C, Li M (2002) UV Raman spectroscopic study on the phase transformation of ZrO_2, Y_2O_3–ZrO_2 and SO_4^{2-}/ZrO_2. J Raman Spectrosc 33:301-308.
33. Guo M, Lu J, Wu Y, Wang Y, Luo M (2011) UV and Visible Raman Studies of Oxygen Vacancies in Rare-Earth-Doped Ceria. Langmuir 27:3872–3877.
34. Dietz RE, Brinkman WF, Meixner AE, Guggenheim HJ (1971) Raman Scattering by Four Magnons in NiO and $KNiF_3$. Phys Rev Lett 27:814.
35. Mironova-Ulmane N, Kuzmin A, Steins I, Grabis J, Sildos I, Pärs M (2007) Raman scattering in nanosized nickel oxide NiO. J Phys Conf Ser 93:012039.
36. George G, Anandhan S (2014) Synthesis and characterisation of nickel oxide nanofibre webs with alcohol sensing characteristics. RSC Adv 4:62009-62020.
37. Budde M, Tschammer C, Franz Ph, Feldl J, Ramsteiner M, Goldhahn R, Feneberg M, Barsan N, Oprea A, Bierwagen O (2018) Structural, optical, and electrical properties of unintentionally doped NiO layers grown on MgO by plasma-assisted molecular beam epitaxy. J Appl Phys 123:195301.

38. Solsona B, Concepcion P, Demicol B, Hernandez S, Delgado JJ, Calvino JJ, López Nieto JM (2012) Selective oxidative dehydrogenation of ethane over SnO_2-promoted NiO catalysts. J Catal 295:104-114.
39. Dupin JC, Gonbeau D, Vinatier Ph, Levasseur A (2000) Systematic XPS studies of metal oxides, hydroxides and peroxides. Phys Chem Chem Phys 2:1319-1324.
40. Haber J (1995) Mechanism of heterogeneous catalytic oxidation, in: R.A. Sheldon, R.A. van Santen (Eds.), in Catalytic Oxidation: Principles and Applications, World Scientific, pp. 17–51.
41. Grasselli RK, Burrington JD, Buttrey DJ, DeSanto Jr. P, Lugmair CG , Volpe Jr. AF, Weingand T (2002) Multifunctionality of active centers in (amm)oxidation catalysts: from Bi–Mo–Ox to Mo–V–Nb–(Te; Sb)–Ox. Top Catal 21: 79–88.
42. Delgado D, Solsona B, Ykrelef A, Rodríguez-Gómez A, Caballero A, Rodríguez-Aguado E, Rodríguez-Castellón E, López Nieto JM (2017) Redox and Catalytic Properties of Promoted NiO Catalysts for the Oxidative Dehydrogenation of Ethane. J. Phys. Chem. C 121:25132−25142.
43. Skoufa Z, Heracleous E, Lemonidou AA (2015) On ethane ODH mechanism and nature of active sites over NiO-based catalysts via isotopic labeling and methanol sorption studies. J Catal 322:118–129
44. Savova B, Loridant S, Filkova D, Millet JMM (2010) Ni-Nb-O catalysts for ethane oxidative dehydrogenation. Appl Catal A-Gen 390: 148-157
45. Zhu H, Ould-Chikh S, Anjum DH, Sun M, Biuasque G, Basset JM, Caps V (2012) Nb effect in the nickel oxide catalyzed low-temperature oxidative dehydrogenation of ethane. J Catal 285:292-303.
46. Delgado D, Sanchís R, Cecilia J A, Rodríguez-Castellón E, Caballero A, Solsona B, López Nieto JM (2019) Support effects on NiO-based catalysts for the oxidative dehydrogenation (ODH) of ethane. Cat Today 333:10-16.
47. Heracleous E, Lee A F, Wilson K, Lemonidou AA (2005) Investigation of Ni-based alumina-supported catalysts for the oxidative dehydrogenation of ethane to ethylene: structural characterization and reactivity studies. J Catal 231: 159-171.
48. Lopez Nieto JM, Coenraads R, Dejoz A, Vazquez MI (1997) The role of metal oxides as promoters of V_2O_5/γ-Al_2O_3 catalysts in the oxidative dehydrogenation of propane. Stud Surf Sci Catal 110: 443-451.

49. Heracleous E, Machli M, Lemonidou AA, Vasalos IA (2005) Oxidative dehydrogenation of ethane and propane over vanadia and molybdena supported catalysts. J Mol Catal A-Chem 232: 29–39.
50. Kung HH, Kung MC (1997) Oxidative dehydrogenation of alkanes over vanadium-magnesium-oxides. Appl Catal A-Gen 157:105-116.
51. Batiot C, Hodnett BK (1996) The role of reactant and product bond energies in determining limitations to selective catalytic oxidations. Appl Catal A-Gen 137:179-191.
52. Moro-oka Y, Ozaki A (1967) The Nature of Adsorbed Olefin on Nickel Oxide as Revealed by a Competitive Reaction Method. J Am Chem Soc 89:5124-5128.
53. Moro-oka Y, Morikawa Y, Ozaki A (1967) Regularity in the Catalytic Properties of Metal Oxides in Hydrocarbon Oxidation. J Catal 7:23-32.

Table 1. Physicochemical and catalytic properties of NiO containing catalysts.

Catalyst	S_{BET} (m^2 g^{-1})	NiO crystal size (nm)[a]	Concentration of O^- (from XPS) at.%	FTIR of adsorbed CO [b]	Catalytic activity [c]	Selectivity to propylene (%) [d]
uNiO	15	35	15.8	2148	87	16
K-NiO	30	17	22.9	-	8.7	11[e]
La-NiO	79	11	14.8	2151	251	28
Al-NiO	n.d	11	n.d.	2155	119	29
Ce-NiO	84	15	11.8	n.d.	923	23
Zr-NiO	120	9	10.5	2155	154	37
Sn-NiO	103	12	10.7	2165	35	36
Nb-NiO	115	9	6.6	2169	59	45

[a)] Mean NiO crystallite sized determined by XRD using the Scherrer equation; [b)] υ(CO) IR band associated to surface Lewis acid sites with acidity higher than that observed on NiO; [c)] Catalytic activity in g_{C3H8} reacted/(kg_{cat} h), determined at 300ºC and using a contact time, W/F, of 8.2 g_{cat} h/mol_{C3H8}; [d)] Selectivity to propylene at 300ºC and 10% propane conversion (modifying the contact time depending on the catalyst); [e)] At 3% conversion as higher conversion could not be achieved due to the low activity of this catalyst.

Table 2. Reaction rate for the oxidation of alkanes and olefins over NiO-based catalysts at 350ºC

Catalyst	Reaction rate[a]		r_{-C2H4}/r_{-C2H6}	Reaction rate[a]		r_{-C3H6}/r_{-C3H8}
	r_{-C2H6}	r_{-C2H4}	*ratio*	r_{-C3H8}	r_{-C3H6}	ratio
uNiO	111	56.1	0.51	140	96.3	0.69
Zr-NiO	134	70.7	0.53	174	111	0.64
Nb-NiO	117	48.8	0.41	130	105	0.81

a) Reaction rate for hydrocarbon conversion, r_{-i}, in 10^4 mol_{hydroc} h^{-1} $(g_{cat})^{-1}$.

Caption to figures

Figure 1. Raman spectra of NiO-based catalysts recorded at an irradiation wavelength of 514 nm (A) and 325 nm (B): a) NiO; b) K-NiO; c) La-NiO; d) Ce-NiO; e) Zr-NiO; f) Sn-NiO; g) Nb-NiO. Characteristics of catalysts in Table 1.

Figure 2. O1s XPS spectra of catalysts: a) NiO; b) K-NiO; c) La-NiO; d) Ce-NiO; e) Zr-NiO; f) Sn-NiO; g) Nb-NiO.

Figure 3. Propane conversion (■) and selectivity to propylene (■) for unpromoted and promoted NiO catalysts during the ODH of propane. Reaction conditions: 325ºC, W/F = 8 g_{cat} h /mol_{C3}. Remaining conditions in the Experimental section. For Ce-NiO catalyst, W/F = 2 g_{cat} h /mol_{C3}.

Figure 4. Variation of the selectivity to propylene at 10% conversion and 350ºC with the amount of adsorbed CO (FTIR). Note: Adsorbed CO total FTIR is the total number of surface acid sites calculated as the number of CO molecules adsorbed on each site.

Figure 5. Influence of amount of electrophilic O^- sites detected by XPS on the selectivity to propylene, during the ODH of propane (○), or on the selectivity to ethylene, during the ODH of ethane (●). Data at 10% alkane conversion and a reaction temperature of 350ºC. Catalytic results for propane ODH (this study), using a C_3/O_2/He molar ratio of 10/10/80; Catalytic results for ethane ODH (from ref. 14), using a C_2/O_2/He molar ratio of 10/3.3/86.7.

Figure 6. Variation of the selectivity to olefin with the alkane conversion at 350ºC during the ODH of propane (A) or the ODH of ethane (B) on Ni-based catalysts: uNiO; Zr-NiO and Nb-NiO. Remaining reaction conditions in text.

Figure 7. Reaction rate for hydrocarbon conversion (r_{-C2H6}, r_{-C3H8}, r_{-C2H4} or r_{-C3H6}, in 10^4 mol_{CxHx} g_{cat}^{-1} h^{-1}) as well as the reaction rate for the formation of the main reaction products (r_{C3H6}, r_{C2H4}, r_{CO2} or r_{CO}, in 10^4 $mol_{product}$ g_{cat}^{-1} h^{-1}) during the oxidation of ethane (**a**), ethylene (**b**), propane (**c**), and propylene (**d**) over NiO, Zr-NiO and Nb-NiO catalysts at 350ºC. Experimental conditions as in Tables S1-S3.

Figure 8. Reaction pattern of the ODH of propane and ethane on NiO based catalysts.

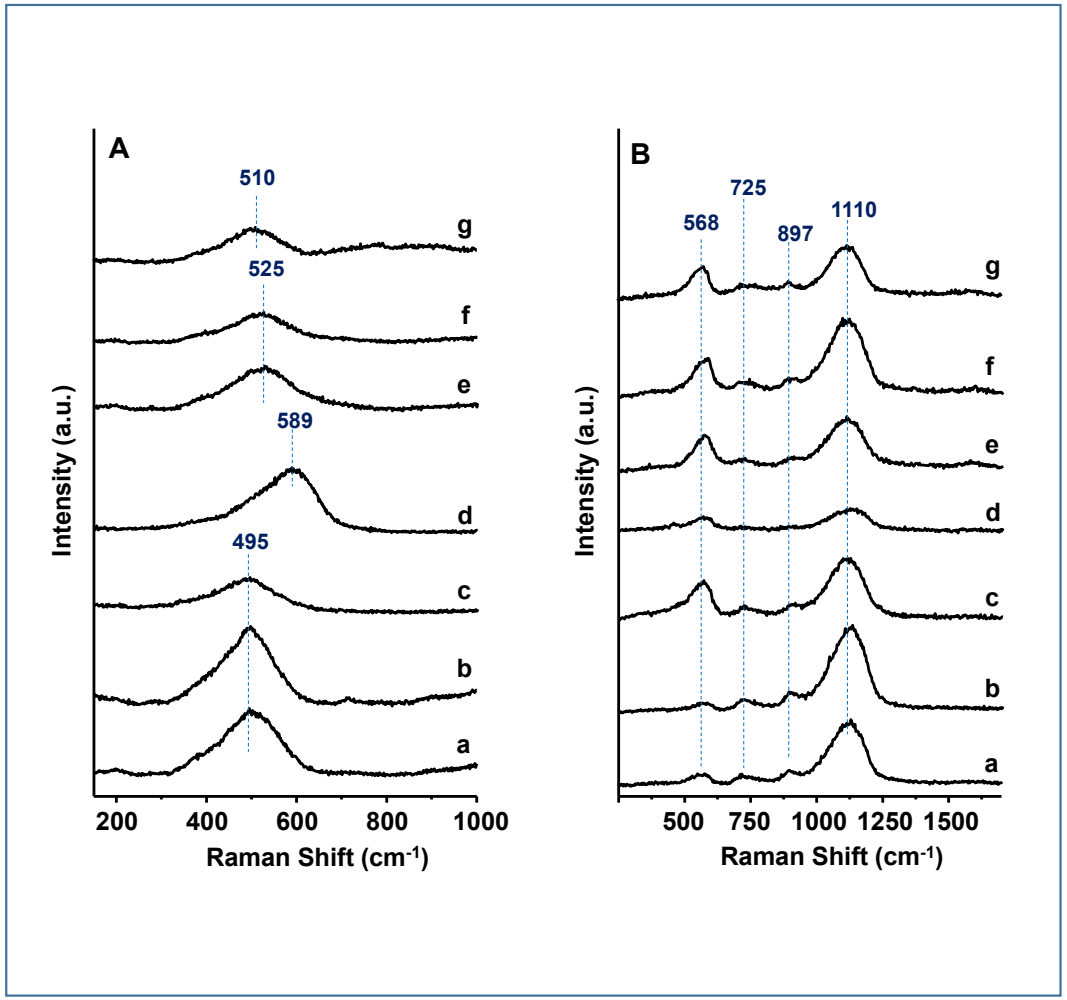
A
510
525
589
495
g
f
e
d
c
b
a
Intensity (a.u.)
200
400
600
800
1000
Raman Shift (cm-1)
B
568
725
897
1110
g
f
e
d
c
b
a
Intensity (a.u.)
500
750
1000
1250
1500
Raman Shift (cm-1)

Fig. 1

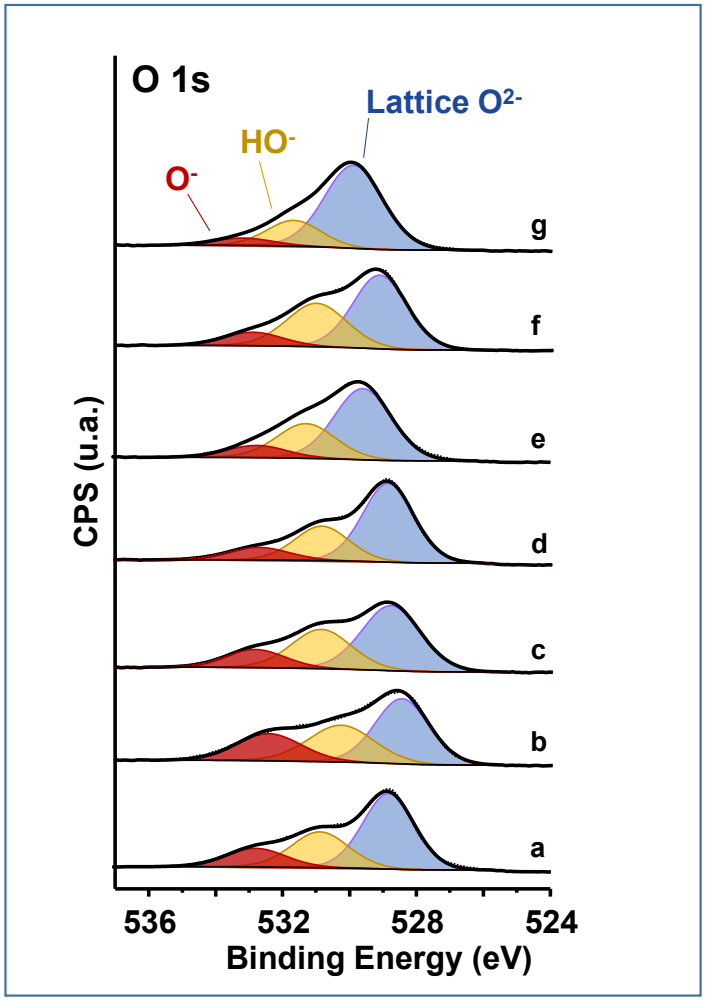
O 1s
Lattice O2-
HO-
O-
g
f
e
d
c
b
a
CPS (u.a.)
536
532
528
524
Binding Energy (eV)

Fig. 2

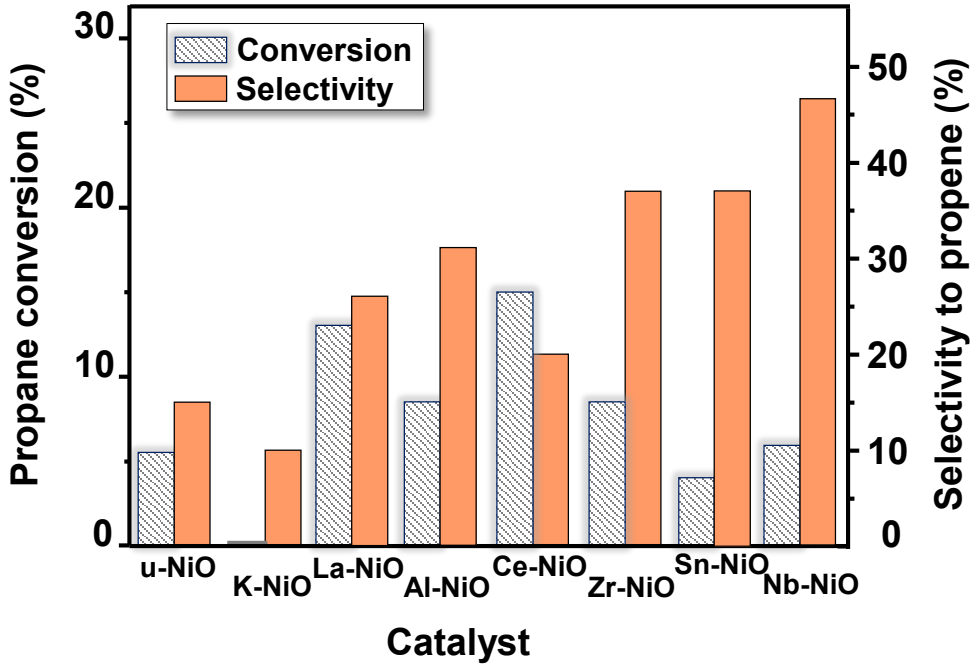
Conversion
Selectivity
Propane conversion (%)
Selectivity to propene (%)
0
10
20
30
0
10
20
30
40
50
u-NiO
K-NiO
La-NiO
Al-NiO
Ce-NiO
Zr-NiO
Sn-NiO
Nb-NiO
Catalyst

Fig. 3

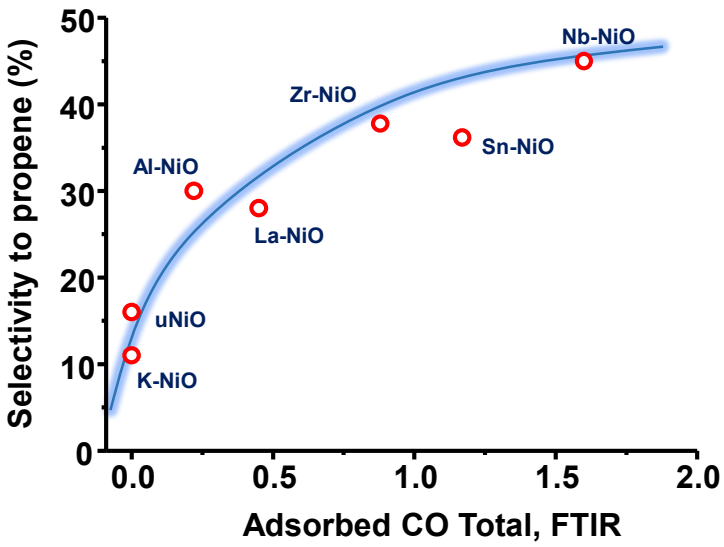
Selectivity to propene (%)
Adsorbed CO Total, FTIR
0
10
20
30
40
50
0.0
0.5
1.0
1.5
2.0
Nb-NiO
Zr-NiO
Sn-NiO
Al-NiO
La-NiO
uNiO
K-NiO

Fig. 4

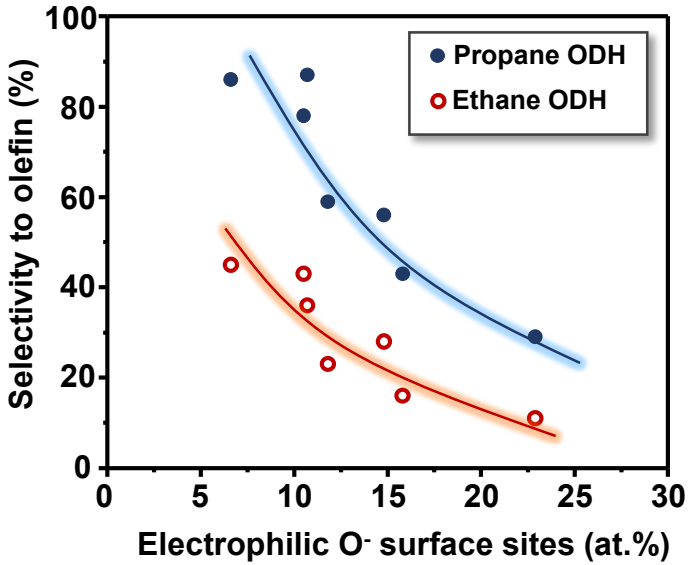
Selectivity to olefin (%)
Electrophilic O- surface sites (at.%)
0
20
40
60
80
100
0
5
10
15
20
25
30
Propane ODH
Ethane ODH

Fig. 5

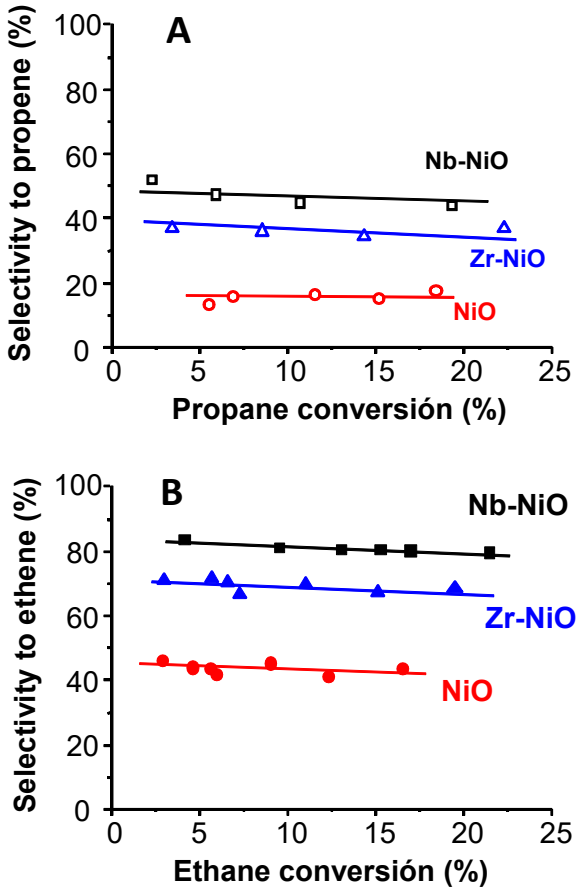
A
Selectivity to propene (%)
Propane conversión (%)
Nb-NiO
Zr-NiO
NiO
B
Selectivity to ethene (%)
Ethane conversión (%)
Nb-NiO
Zr-NiO
NiO

Fig. 6

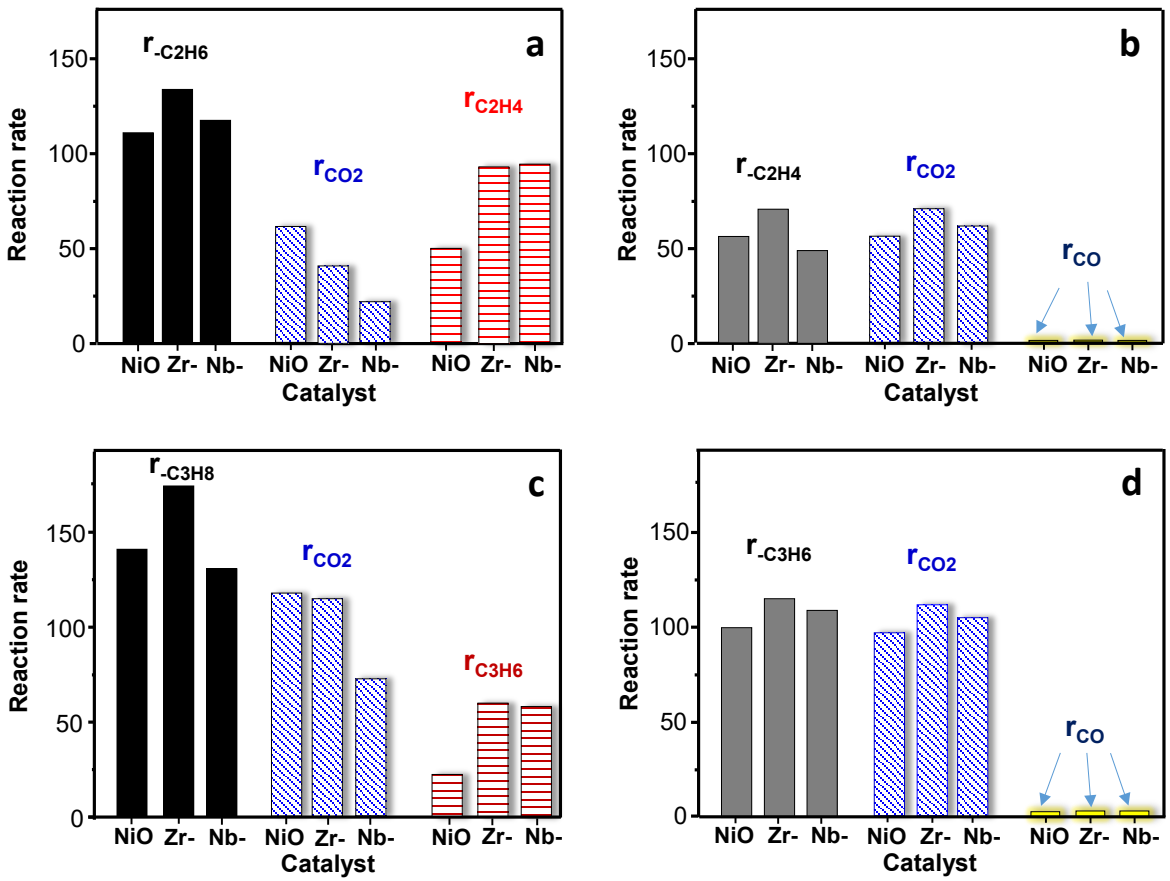
a
b
c
d
Reaction rate
Catalyst
NiO Zr- Nb-
r-C2H6
rC2H4
rCO2
r-C2H4
rCO
r-C3H8
rC3H6
r-C3H6

Fig. 7

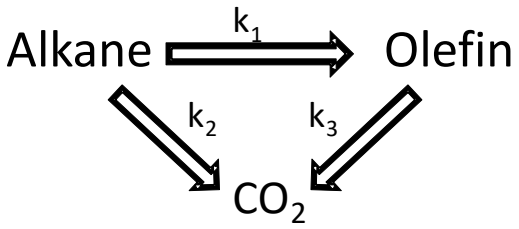

Figure 8. Reaction network of the ODH of propane or ethane on NiO based catalysts.